DOI: 10.1534/genetics.110.124883

Regulation of Anoxic Death in *Caenorhabditis elegans* by Mammalian Apoptosis Signal-Regulating Kinase (ASK) Family Proteins

Teruyuki Hayakawa,* Kumiko Kato,* Ryoichi Hayakawa,* Naoki Hisamoto,† Kunihiro Matsumoto,† Kohsuke Takeda*,[1] and Hidenori Ichijo*,[1]

**Laboratory of Cell Signaling, Graduate School of Pharmaceutical Sciences, Strategic Approach to Drug Discovery and Development in Pharmaceutical Sciences, Global Center of Excellence Program, and Core Research for Evolutional Science and Technology, Japan Science and Technology Corporation, The University of Tokyo, 7-3-1 Hongo, Bunkyo-ku, Tokyo 113-0033, Japan and* †*Group of Signal Transduction, Laboratory of Cell Regulation, Division of Biological Science, Graduate School of Science, Nagoya University, Chikusa-ku, Nagoya 464-8602, Japan*

Manuscript received November 2, 2010
Accepted for publication December 25, 2010

ABSTRACT

Cells and organisms face anoxia in a wide variety of contexts, including ischemia and hibernation. Cells respond to anoxic conditions through multiple signaling pathways. We report that NSY-1, the *Caenorhabditis elegans* ortholog of mammalian apoptosis signal-regulating kinase (ASK) family of MAP kinase (MAPK) kinase kinases (MAP3Ks), regulates viability of animals in anoxia. Loss-of-function mutations of *nsy-1* increased survival under anoxic conditions, and increased survival was also observed in animals with mutations in *tir-1* and the MAPK kinase (MAP2K) *sek-1*, which are upstream and downstream factors of NSY-1, respectively. Consistent with these findings, anoxia was found to activate the p38 MAPK ortholog PMK-1, and this was suppressed in *nsy-1* and *tir-1* mutant animals. Furthermore, double-mutant analysis showed that the insulin-signaling pathway, which also regulates viability in anoxia, functioned in parallel to NSY-1. These results suggest that the TIR-1–NSY-1–SEK-1-PMK-1 pathway plays important roles in the reponse to anoxia in *C. elegans*.

HYPOXIC (low oxygen concentration, for example, 0.5 or 1%) or anoxic (no oxygen) conditions are observed in mammalian pathogenic tissues such as solid tumors or ischemic regions and during embryonic development, when the circulation system is not mature yet (Brahimi-Horn and Pouyssegur 2007; Dunwoodie 2009). Hypoxia-inducible factors (HIFs), which are evolutionarily conserved transcription factors, have been reported to play pivotal roles in oxygen homeostasis and hypoxic survival responses, especially at the transcription levels (Semenza 2003). In *C. elegans*, *hif-1* loss-of-function mutant animals show hypersensitivity to hypoxia (Epstein *et al.* 2001; Jiang *et al.* 2001; Padilla *et al.* 2002). However, *hif-1* mutant animals do not show a lower survival rate under anoxic conditions (Padilla *et al.* 2002), suggesting that hypoxia and anoxia may affect the viability of animals through different molecular mechanisms (Powell-Coffman 2010). Under anoxic conditions, nematodes decrease their metabolic rate and arrest their cell cycle progression (Padilla *et al.* 2002). Over the last decade, several studies have examined the mutations that affect the survival rate under lethal anoxia (Scott *et al.* 2002; Nystul *et al.* 2003; Mendenhall *et al.* 2006; Samokhvalov *et al.* 2008; Anderson *et al.* 2009; Mabon *et al.* 2009; Menuz *et al.* 2009), but the signaling pathways that regulate survival under anoxic conditions have not fully been elucidated.

Mammalian apoptosis signal-regulating kinase (ASK) family proteins are MAP kinase (MAPK) kinase kinases (MAP3Ks) of the c-Jun N-terminal kinase (JNK) and p38 MAPK pathways and play pivotal roles in cellular responses to various stresses such as oxidative stress and endoplasmic reticulum (ER) stress (Ichijo *et al.* 1997; Takeda *et al.* 2008). *C. elegans* possesses a single ASK family protein, named NSY-1, and its functions are well conserved with those of mammalian ASK1. NSY-1 was originally identified as a regulator of neuronal cell fate (Sagasti *et al.* 2001). In 2002, Kim *et al.* (2002) demonstrated that NSY-1 and its downstream MAPK kinase (MAP2K) SEK-1 and MAPK PMK-1 were indispensable for the immune response to various bacterial infections, including *Pseudomonas aeruginosa*. In addition, *nsy-1* mutant animals have been reported to show sensitivity to gram-positive bacteria *Staphylococcus aureus* with a defect in germline apoptosis (Sifri *et al.* 2003), sensitivity to oxidative stress (Kondo *et al.* 2005), resistance to germline apoptosis upon arsenite or cadmium stimulation (Pei *et al.* 2008; Wang *et al.* 2008) and

Supporting information is available online at http://www.genetics.org/cgi/content/full/genetics.110.124883/DC1.

[1]*Corresponding authors:* Laboratory of Cell Signaling, Graduate School of Pharmaceutical Sciences, The University of Tokyo, 7-3-1 Hongo, Bunkyo-ku, Tokyo 113-0033, Japan.
E-mail: takeda@mol.f.u-tokyo.ac.jp and ichijo@mol.f.u-tokyo.ac.jp

a defect in egg laying (Shivers *et al.* 2009). These phenotypes of *nsy-1* mutant animals strongly suggest that NSY-1 plays important roles in stress responses in *C. elegans*. Here we show that a loss-of-function mutation of *nsy-1* increases the survival rate under anoxic but not hypoxic conditions.

MATERIALS AND METHODS

Maintenance and strains of *C. elegans*: Maintenance and genetic manipulation of *C. elegans* were carried out as described previously (Brenner 1974). The following mutations on N2 background were used: *nsy-1(ky400)*, *nsy-1(ag3)*, *nsy-1(ok593)*, *nsy-1(tm850)*, *sek-1(km4)*, *pmk-1(km25)*, *kgb-1(km21)*, *jnk-1(gk7)*, *tir-1(tm3036)*, *hif-1(ia04)*, *daf-2(e1370)*, and *daf-16(mgDf47)*. All experiments were carried out at 20° unless otherwise noted. The alkaline bleach method was used for synchronization.

Stress assays: For all stress assays, the graphs presented in the figures show the combined data from biologically independent experiments. The numbers of independent trials and statistical indexes are indicated in each figure legend.

For the assay of oxidative stress, synchronized L1 larvae were cultured on nematode growth medium (NGM) plates containing 0.4 mm paraquat (Tokyo Chemical Industry, Tokyo, Japan) seeded with OP50. Ninety-six hours later, animals in the L4 larval and adult stages were counted as surviving animals. Each assay was performed in triplicate ($n > 50$ animals per plate).

For the assay of ER stress, synchronized L1 larvae were cultured on NGM plates containing 5 μg/ml tunicamycin (Wako, Osaka, Japan) seeded with OP50. Seventy-two hours later, animals in the L4 larval and adult stages were counted as surviving animals. Each assay was performed in triplicate ($n >$ 50 animals per plate).

For the assay of high salt stress, synchronized young adult animals were transferred onto NGM plates seeded with OP50 containing an additional 0.4 m sodium chloride (Wako). Twenty-four hours later, animals that moved spontaneously or responded to platinum wire touch were considered surviving animals. Each assay was performed with 20 animals.

To analyze the effects of a DNA-damaging reagent, adult animals were left on NGM plates seeded with OP50 containing 0.1 mg/ml methyl methanesulfonate (Sigma, St. Louis, MO) to lay eggs for 24 hr. Then, the adult animals were removed and the total number of laid eggs was counted. Twenty-four hours later, the number of hatched animals was counted to determine the survival rate. Each assay was performed with >100 animals.

For life span analysis, synchronized L4 animals were transferred onto NGM plates containing 0.1 mg/ml 5-fluoro-2′-deoxyuridine (FUDR; Sigma) seeded with OP50. FUDR was used to inhibit germline proliferation because *nsy-1(ky400)* mutant animals showed a mild egg-laying defect phenotype and consequently the hatched larvae killed their parents, which is also known as "bagging" phenotype (Shivers *et al.* 2009). Animals were checked for survival every 2 or 3 days. Animals that moved spontaneously or responded to platinum wire touch were counted as surviving animals. The assay was performed once in triplicate ($n > 50$ animals per plate) and the data were combined to draw a single survival curve.

To analyze the effects of anoxia, synchronized young adult animals on "low nematode growth medium (LNGM)" plates (containing 30% of peptone as normal NGM plates) seeded with OP50 were packed into a plastic bag containing an Anaerocult A mini sachet (Merck, Rahway, NJ). After anoxic incubation, LNGM plates were exposed to normoxic conditions for 24 hr so that the number of surviving animals could be counted, because *C. elegans* animals enter a "suspended animation" state in which they stop locomotion. Animals that moved spontaneously or responded to platinum wire touch were counted as surviving animals. Anoxic states were monitored using Anaerotest strips (Merck). The graphs presented in the figures show the mean survival rate from biologically independent experiments. We could not avoid the variability of the absolute values of survival rates between experiments, possibly because of slight differences in the culture conditions of animals and/or lot-to-lot variations of reagents, *e.g.*, Anaerocult A mini. We therefore repeated the same experiments within a few weeks, which could minimize such variability. Each assay was performed in triplicate ($n > 50$ animals per plate except for the rescue experiments, which used $n > 20$ animals per plate).

To examine the survival in 20% CO_2, synchronized young adult animals on NGM plates seeded with OP50 were cultured in 20% CO_2 at 28° in a CO_2 incubator (ESPEC BNA-111). The animals that moved spontaneously or responded to platinum wire touch were counted as surviving animals. The assay was performed with 20 animals. The data shown are representative of two independent experiments.

To examine the effects of sodium azide (NaN_3), ~100 synchronized young adult animals were collected, incubated with various concentrations of sodium azide in M9 for 10 hr, and then spread on NGM plates seeded with OP50. Twenty-four hours later, the animals that moved spontaneously or responded to platinum wire touch were counted as surviving animals. The experiments were performed five times.

RNA interference experiments: To test the survival rate under anoxia by an RNAi experiment, we used an L1-soaking method (Sugimoto 2006). We chose this method both because it could be easily combined with our anoxia assay in which the alkaline bleach method is used and because the feeding RNAi method ended in failure, since feeding on the *Escherichia coli* strain HT115 dramatically increased the survival rate under anoxia, which masked the change of survival rate by *nsy-1* RNAi and mutation (data not shown). dsRNA preparation and soaking were carried out as described previously (Sugimoto 2006). Briefly, synchronized L1 larvae were treated with dsRNA for 48 hr. Template DNA for dsRNA synthesis were amplified by PCR using the following primers: for gfp, 5′-GCGTAATACGACTCACTATAGGGATGAGTAAAG GAGAAGAACTTT-3′ and 5′-GCGTAATACGACTCACTATA GGGTAGTTCATCCATGCCATGTGTA-3′; for *nsy-1*, 5′-GCGT AATACGACTCACTATAGGGTGAAGCAGCTTTGATGATGG -3′ and 5′-GCGTAATACGACTCACTATAGGGTTCGGTTACT GGATTCAGCC-3′.

Rescue experiments: The general methods used for generating transgenic animals that possess extrachromosomal DNA arrays were as described previously (Mello *et al.* 1991). *nsy-1* cDNA (Sagasti *et al.* 2001) fused with gfp was subcloned to the region downstream of the *dpy-7*, *vha-6*, and *unc-119* promoters to form a hypodermal, intestinal, and neuronal rescue construct, respectively (Oka *et al.* 2001; Lesa *et al.* 2003; Moribe *et al.* 2004). The *dpy-7* and *vha-6* constructs were injected into *nsy-1(ky400)* mutant animals at a concentration of 5 μg/ml together with the marker construct *vha-6::gfp* at 50 μg/ml. The *unc-119* construct was injected into *nsy-1(ky400)* mutant animals at a concentration of 50 μg/ml.

Immunoblotting: For immunoblotting, ~100 synchronized young adult animals per lane were immediately harvested using M9 buffer, frozen by liquid nitrogen, and lysed with the same volume of RIPA buffer (50 mm Tris-HCl pH 8.0, 150 mm NaCl, 1% Nonidet P-40, 0.5% sodium deoxycholate, 0.1% SDS, 5 mg/ml Aprotinin, and 1 mm phenylmethyl sulfonyl fluoride) on ice. The lysates were added to the same volume of

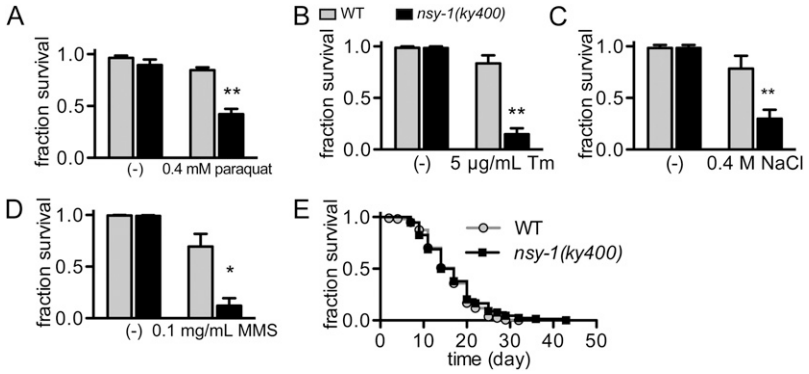

FIGURE 1.—*nsy-1* mutant animals are susceptible to various stresses. (A–D) Survival rates of wild-type (WT) and *nsy-1(ky400)* mutant animals cultured on NGM plates containing (A) 0.4 mM paraquat for oxidative stress, (B) 5 μg/ml tunicamycin (Tm) for ER stress, (C) additional 0.4 M NaCl for high salt stress, and (D) 0.1 mg/ml methyl methanesulfonate (MMS) as a DNA-damaging reagent. Data represent the mean (± SEM) of the survival fraction from three independent experiments. $^{**}P < 0.01$ and $^{*}P < 0.05$ by unpaired Student's *t*-test. (E) Life span curve of WT and *nsy-1(ky400)* mutant animals on NGM plates containing 0.1 mg/ml 5-fluoro-2′-deoxyuridine. Data represent the survival fraction of triplicate plates from the same preparation ($n > 50$ animals per plate). $P = 0.237$ by the log-rank test.

2× SDS sample buffer (40 mM Tris-HCl pH 8.8, 80 μg/ml bromophenol blue, 28.8% glycerol, 4% SDS, and 20 mM DTT), boiled at 98° for 5 min, subjected to SDS–PAGE, and transferred to BioTrace PVDF membranes (Pall, Port Washington, NY). The antibodies used were antiphospho-p38 MAPK (rabbit polyclonal; Cell Signaling Technology, Beverly, MA), anti-PMK-1 (KIM *et al.* 2002) and anti-actin (AC40; Sigma). For the quantification of PMK-1 activity, the band intensity of the phospho-p38 blot was quantified using ImageJ software (National Institutes of Health, Bethesda, MD; http://rsb.info.nih.gov/ij/) and divided by that of the actin blot. Data were normalized using the signal from the wild type (WT) at 24 hr as one. The immublots of seven independent experiments were quantified. For *N*-acetylcysteine (Nac) pretreatment, Nac was added to the NGM plates after synchronization at a concentration of 5 mM.

Oxygen consumption: Oxygen consumption rates were monitored as described previously (SRINIVASAN *et al.* 2008) with slight modifications. Briefly, ~300 synchronized young adult animals fed with OP50 were deposited in a single well of a 96-well format Oxygen Biosensor System (BD Biosciences, San Jose, CA) using S basal buffer. Plates were incubated at 20° and fluorescent intensities were measured every 30 min for 3 hr. The intensity after 2 hr of incubation, when the signal was saturated, was used for calculating the oxygen consumption rate. Raw fluorescent intensities from experimental wells were divided by the blank signal of the corresponding well for normalization. The graph in supporting information, Figure S4 shows average oxygen consumption rates from four independent experiments performed in duplicate.

RESULTS

***nsy-1* mutant animals showed a lower survival rate under various stresses:** To explore the evolutionarily conserved functions of ASK family proteins in stress responses, we analyzed the phenotypes of *C. elegans nsy-1* loss-of-function mutant animals. In previous reports on stress response, *nsy-1* mutant animals showed a lower survival rate than their wild-type counterparts under bacterial infection and oxidative stress (KIM *et al.* 2002; SIFRI *et al.* 2003; KONDO *et al.* 2005). We first reproduced that the *nsy-1(ky400)* strain, which has a mutation resulting in a premature stop codon before the kinase domain, had a lower survival rate under oxidative stress induced by paraquat (Figure 1A). In addition, *nsy-1(ky400)* mutant animals showed susceptibility to the ER stress-inducer tunicamycin, high salt stress, and the DNA-damaging reagent methyl methanesulfonate (Figure 1, B–D). Since *nsy-1(ky400)* mutant animals showed almost the same survival curve as wild-type animals under non-stressed conditions (Figure 1E), the lower survival rate of *nsy-1(ky400)* mutant animals observed under the stressed conditions may be ascribable to a defect of the appropriate responses to these stresses.

***nsy-1* mutant animals showed a higher survival rate under anoxia:** To our surprise, the *nsy-1(ky400)* mutant animals showed a higher survival rate than the wild-type ones in anoxia (Figure 2A). Three additional loss-of-function alleles of *nsy-1* (*ag3*, *ok593*, and *tm850*) also showed similar higher survival rates than the wild-type allele (Figure 2B). A reduction of the *nsy-1* transcript by RNAi also resulted in an increase of the survival rate in anoxia (Figure 2C). These results strongly suggest that the *nsy-1(ky400)* mutant shows prolonged survival in anoxia. This phenotype was rescued by extrachromosomally introduced transgenes that express NSY-1 in the hypodermal, intestinal, or neuronal tissues (Figure 2, D and E), suggesting that NSY-1 non-cell autonomously regulates the organismal death or that NSY-1 might play roles in each of these tissues that contribute to the organismal death.

We next examined the survival rate under 20% CO_2 concentration because we used the catalyst Anaerocult A mini, which converts oxygen (O_2) to carbon dioxide (CO_2) to establish anoxic conditions. We found that animals did not die under the 20% CO_2 conditions within 120 hr, eliminating the possibility that animal death under Anaerocult A mini was caused by the increase in CO_2 concentration (Figure 2F).

To examine whether the prolonged-survival phenotype is caused by hypoxia or anoxia, we analyzed the survival rate of *hif-1* mutant animals in Anaerocult A mini; *hif-1(ia04)* mutant animals did not show a lower survival rate in the Anaerolcult A mini culture than wild-type ones (Figure 2G). Because *hif-1(ia04)* mutant has been reported to show a lower survival rate in hypoxia (0.5 or 1% O_2),

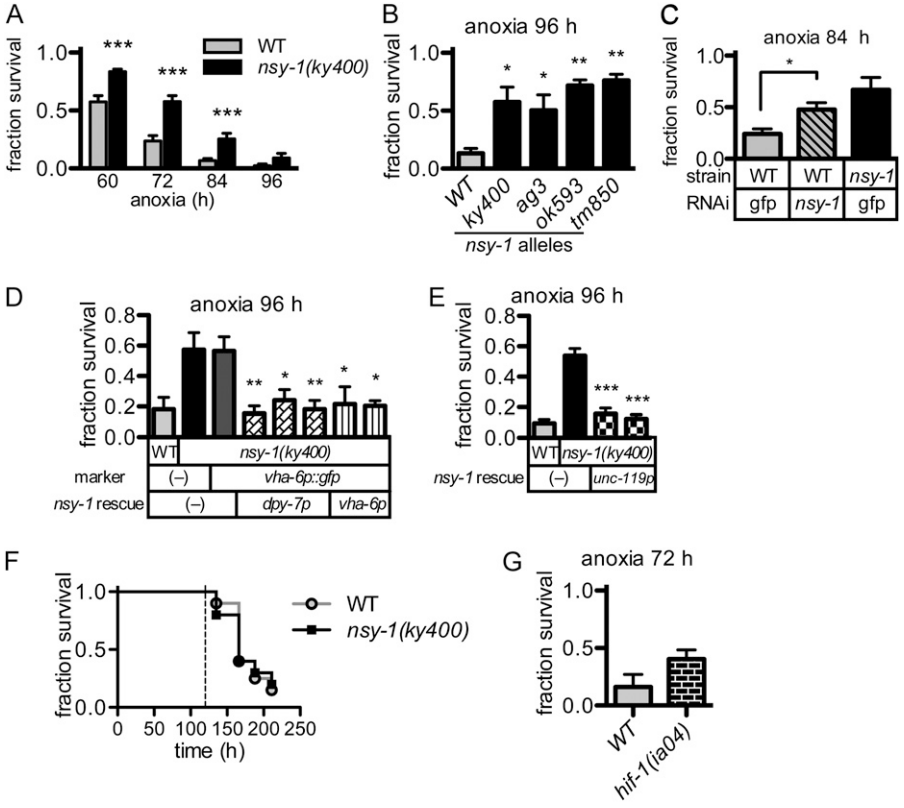

FIGURE 2.—*nsy-1* mutant animals show a higher survival rate under anoxia. (A) The survival rates of WT and *nsy-1(ky400)* mutant animals incubated with Anaerolcult A mini for the indicated periods and recovered under normoxia for 24 hr. Animals that moved spontaneously or responded to platinum wire touch were counted as surviving animals. Data represent the mean (± SEM) survival fraction from 22 independent experiments. $***P < 0.001$ by unpaired Student's *t*-test at each time point. (B) Survival rates of WT and four *nsy-1* loss-of-function alleles in anoxia. Data represent the mean (± SEM) survival fraction from three independent experiments. $*P < 0.05$ and $**P < 0.01$ by one-way analysis of variance and Dunnett's multiple comparison test compared with the WT. (C) Survival rate of *nsy-1(RNAi)* animals in anoxia. Data represent the mean (± SEM) survival fraction from three independent experiments. $*P < 0.05$ by unpaired Student's *t*-test. (D) Survival rate under condition of anoxia of transgenic animals that possessed a hypodermal and intestinal expression construct in the *nsy-1(ky400)* genetic background. Each bar indicates the independent transgenic line. Data represent the mean (± SEM) survival fraction from three independent experiments. $**P < 0.01$ and $*P < 0.05$ by one-way analysis of variance and Dunnett's multiple comparison test compared with *nsy-1(ky400)* with *Ex[vha-6p::gfp]* marker only (third column). (E) Survival rate under condition of anoxia of transgenic animals that possessed a neuronal expression construct in the *nsy-1(ky400)* genetic background. Each bar indicates the independent transgenic line. Data represent the mean (± SEM) survival fraction from three independent experiments. $***P < 0.001$ by one-way analysis of variance and Dunnett's multiple comparison test compared with *nsy-1(ky400)* without the transgene (second column). (F) Survival curve of WT and *nsy-1(ky400)* mutant animals incubated in 20% CO_2 conditions at 28°. The broken line indicates the maximum time range of induced anoxia in the present study. Assay was performed once with 20 animals. $P = 0.842$ by the log-rank test. (G) Survival rate of *hif-1(ia04)* mutant animals incubated with Anaerocult A mini. Data represent the mean (± SEM) survival fraction from four independent experiments. $P = 0.122$ by unpaired Student's *t*-test.

but not in anoxia (0% O_2) (JIANG *et al.* 2001; PADILLA *et al.* 2002), the animal death under Anaerocult A mini appears to be due to anoxia rather than hypoxia.

The TIR-1–NSY-1–SEK-1–PMK-1 pathway plays a major role in anoxic death: Next we assessed the involvement of the known upstream and downstream signaling components of NSY-1 in the anoxic response (Figure 3A). A mutation in the TIR domain-containing adaptor protein TIR-1, which has been shown to be involved in both neuronal differentiation (CHUANG and BARGMANN 2005) and innate immunity (COUILLAULT *et al.* 2004; LIBERATI *et al.* 2004) upstream of NSY-1, increased the survival rate in anoxia (Figure 3B), suggesting that TIR-1 functions as an upstream regulator of NSY-1 also in the anoxic response.

To examine whether the phenotype of the *nsy-1* mutant is dependent on the MAP kinase pathways, animals with mutations of components of the p38 MAPK and JNK pathways were analyzed. The survival rate of animals with a mutation in *sek-1*, the sole MAP2K that has been reported to function downstream of NSY-1 (KIM *et al.* 2002; TANAKA-HINO *et al.* 2002), was higher than that of their wild-type counterparts, suggesting that SEK-1 plays a major role in the anoxic response downstream of NSY-1 (Figure 3C). On the other hand, we could not specify the responsible MAPKs, since neither mutant animals of one of three MAPKs of the p38 pathway, *pmk-1(km25)*, nor those of the MAPKs of the JNK pathway, *kgb-1(km21)* and *jnk-1(gk7)*, showed significantly higher survival rates than wild-type ones probably because of functional redundancy among MAPKs (Figure 3D).

Nevertheless, since PMK-1 is the only MAPK that has been reported to function downstream of NSY-1 and SEK-1 in *C. elegans* (KIM *et al.* 2002; TANAKA-HINO *et al.* 2002), we examined biochemically the involvement of PMK-1 in the anoxic response downstream of NSY-1 and SEK-1. We used a phospho-specific p38 MAPK antibody to monitor the PMK-1 activity, since the amino acid sequences around the activating phosphorylation sites are well conserved from *C. elegans* to mammals (Figure S1). We found that anoxia induced PMK-1 activation,

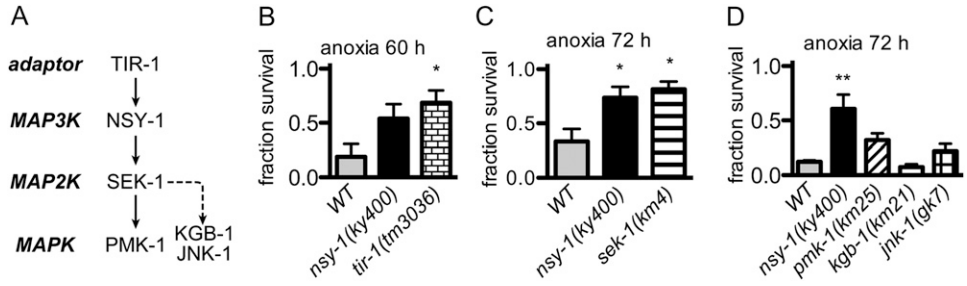

FIGURE 3.—The TIR-1–NSY-1–SEK-1 pathway is required for anoxic death. (A) Drawing of the MAP kinase pathways tested in this study. Survival rate of animals with a mutation in (B) *tir-1(tm3036)*, an upstream adaptor protein of NSY-1, (C) *sek-1(km4)*, the single MAP2K of the p38 pathway, and (D) *pmk-1(km25)*, *kgb-1(km21)*, and *jnk-1(gk7)*, MAPKs of the p38 and JNK pathways. Data represent the mean (± SEM) of the survival fraction from three (B and C) or four (D) independent experiments. $^{**}P < 0.01$ and $^{*}P < 0.05$ by one-way analysis of variance and Dunnett's multiple comparison test compared with WT, respectively.

which was suppressed in *nsy-1* mutant (Figure 4, A and B). The total amount of PMK-1 was assessed by an anti–PMK-1 antibody (Figure S2), and little difference was observed between the wild-type and *nsy-1(ky400)* mutant animals under the basal and stimulated conditions. These results suggest that the NSY-1–SEK-1–PMK-1 pathway operates in the anoxic response. Moreover, PMK-1 activation in response to anoxia was also suppressed in the *tir-1(tm3036)* mutant (Figure 4C), suggesting that TIR-1 is an important upstream factor of the NSY-1–SEK-1–PMK-1 pathway.

Reactive oxygen species (ROS) are produced when anoxic cells are exposed to normoxic conditions, a phenomenon known as "reoxygenation." Pretreatment of wild-type animals with *N*-acetylcysteine (Nac) suppressed the PMK-1 activation induced by the ROS-inducer hydrogen peroxide, but not by anoxia, suggesting that ROS are not involved in PMK-1 activation by anoxia (Figure 4D).

NSY-1 functions independently of the insulin-signaling pathway: Since a mutation in the *daf-2* gene, which encodes the insulin/insulin-like growth factor receptor, is known to result in increased resistance to anoxia (SCOTT *et al.* 2002; MENDENHALL *et al.* 2006), we evaluated the possible genetic interactions between *nsy-1* and the components of the insulin pathway. *nsy-1;daf-2* double-mutant animals showed a higher survival rate than their respective single mutants, suggesting that *nsy-1* and *daf-2* function in parallel (Figure 5A). We next asked whether the activation of PMK-1 in *daf-2(e1370)* mutant animals would also be suppressed like that in *nsy-1(ky400)*. If *daf-2* lies upstream of the NSY-1–SEK-1–PMK-1 pathway, the activation of PMK-1 in response to anoxia should be suppressed, because both the *daf-2(e1370)* and *nsy-1(ky400)* mutants had higher survival rates than their wild-type counterparts. However, anoxia-induced PMK-1 activation in *daf-2(e1370)* mutant animals was not suppressed but rather elevated, suggesting that *daf-2* does not lie upstream of the NSY-1–SEK-1–PMK-1 pathway at least in anoxia-induced PMK-1 activation (Figure 5B). In addition, a mutation in the Forkhead family transcription factor *daf-16*, which suppresses increased resistance of *daf-2* mutant animals to anoxia (SCOTT *et al.* 2002; MENDENHALL *et al.* 2006), did not suppress the

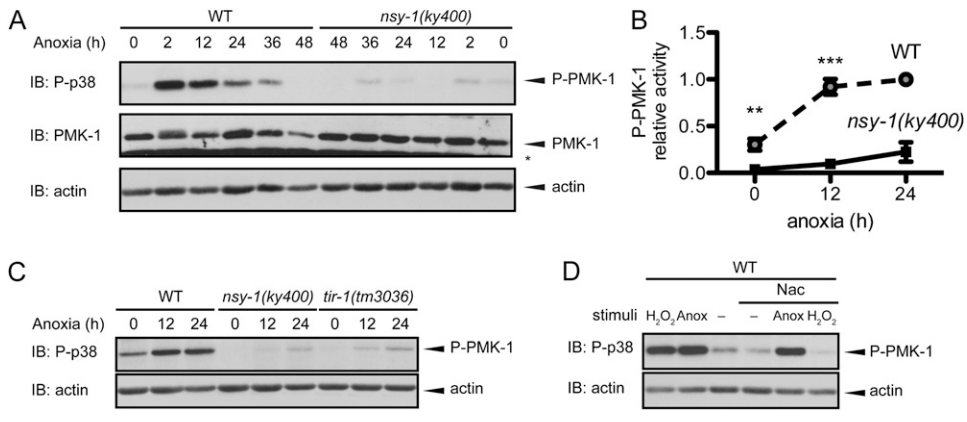

FIGURE 4.—The TIR-1–NSY-1–SEK-1–PMK-1 pathway is activated in response to anoxia. (A) PMK-1 activities in the WT and *nsy-1(ky400)* mutant animals in anoxia were measured by immunoblotting (IB) using a phospho-specific p38 (P-p38) antibody. An asterisk indicates a nonspecific band. Anti-actin was used as a loading control. The data shown are representative of three independent immunoblots. (B) Quantification of phospho-PMK-1 band intensities at 0, 12, and 24 hr in the same experiment as in A. For the quantification of PMK-1 activity, the band intensity of the phospho-p38 blot was quantified and divided by that of the actin blots. Data represent the mean (± SEM) relative phospho-PMK-1 activity from seven independent experiments. $^{**}P < 0.01$ and $^{***}P < 0.001$ by unpaired Student's *t*-test at each time point. (C) PMK-1 activities in the WT, *nsy-1(ky400)*, and *tir-1(tm3036)* mutant animals in anoxia were measured by IB. The data shown are representative of three independent immunoblots. (D) PMK-1 activities in the *N*-acetylcysteine (Nac)-pretreated WT animals stimulated by 1 mM of hydrogen peroxide (H_2O_2) or anoxia (Anox) were measured by immunoblotting. The data shown are representative of two independent immunoblots.

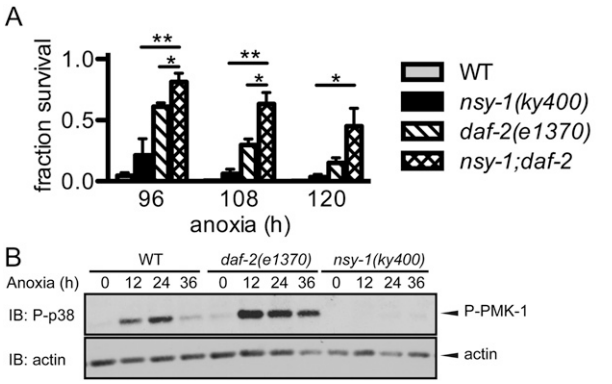

FIGURE 5.—NSY-1 functions independently of the insulin-signaling pathway. (A) Survival rate of WT, *nsy-1(ky400)*, *daf-2(e1370)*, and *nsy-1(ky400);daf-2(e1370)* double-mutant animals under anoxia. Data represent the mean (± SEM) survival fraction from four independent experiments. $^{**}P < 0.01$ and $^{*}P < 0.05$ by unpaired Student's *t*-test. (B) Anoxia-induced PMK-1 activation in *daf-2(e1370)* mutant animals was measured by immunoblotting (IB). The data shown are representative of four independent immunoblots. (C) Survival rate of WT, *nsy-1(ky400)*, *daf-16(mgDf47)*, and *nsy-1(ky400);daf-16(mgDf47)* double-mutant animals under condition of anoxia. Data represent the mean (± SEM) survival fraction from three independent experiments. $^{**}P < 0.01$ and $^{*}P < 0.05$ by unpaired Student's *t*-test of WT and *daf-16(mgDf47)* backgrounds, respectively.

increased resistance to anoxia of *nsy-1* mutant animals (Figure 5C). Taken together, these results indicate that the NSY-1–SEK-1–PMK-1 pathway comprises a pathway that functions independently of the insulin pathway in anoxic responses.

DISCUSSION

In this report, we have shown that *C. elegans* with mutations in the TIR-1–NSY-1–SEK-1 pathway showed a higher survival rate than wild-type animals in anoxia (Figures 2A and 3, B and C). Since the metabolic inhibitor sodium azide is widely used as an anoxia mimetic, we examined whether the *nsy-1* loss-of-function mutation protects against death induced by sodium azide. However, we did not observe any difference in the survival rate between wild-type and *nsy-1* mutant animals, while *daf-2* mutant animals were resistant to the sodium azide as previously reported (SCOTT *et al.* 2002) (Figure S3). The discrepancy between the response to anoxia and to sodium azide may be due to the variety of the effects caused by sodium azide, such as cytosolic acidification and energy failure.

Recently, the transcription factor ATF-7 has been reported to be regulated by the NSY-1–SEK-1–PMK-1 pathway in the context of innate immunity (SHIVERS *et al.* 2010). If some of the pathogen-induced genes regulated by ATF-7 are also induced by anoxia, the mechanisms by which animals respond to pathogenic bacteria and anoxia would be at least partly the same. SKN-1 is another transcription factor that has been reported to be regulated by PMK-1; in the case of SKN-1, the regulation by PMK-1 was shown to occur in response to arsenite stimulation (INOUE *et al.* 2005). Although we have not directly examined the survival rate of the *skn-1* mutant because of its lethality, the transcription levels of *skn-1* target genes (for example, *gcs-1*) were not elevated upon anoxic treatment. In both cases, however, loss of *sek-1* resulted in a decrease in the survival rate in the presence of pathogenic bacteria or arsenite stimulation, which is the opposite of the phenotype observed in this study.

Under anoxic conditions, *C. elegans* decreases its metabolic rate (VAN VOORHIES and WARD 2000). In contrast to *daf-2* mutant animals, which have been reported to exhibit lower O_2 consumption than their wild-type counterparts (VAN VOORHIES and WARD 1999), *nsy-1* mutant animals showed an O_2 consumption rate comparable to that of the wild-type animals (Figure S4). This result suggests that the metabolic rates of the wild-type and *nsy-1* mutant animals have little to do with their survival phenotypes in anoxia.

What advantage do animals gain by activating this pathway, which, in the end, only results in anoxic death? One possibility is that NSY-1–dependent responses contribute to survival at an earlier stage in anoxia but reciprocally change their role to contribute to anoxic death at a later stage. This assumption corresponds to the fact that PMK-1 activation in response to anoxia is observed within 36 hr, which is earlier than the time course of anoxic death (Figure 4A). The band intensity of phospho-PMK-1 then decreases, perhaps due to the depletion of intracellular ATP. Another possibility is that NSY-1–dependent survival responses to anoxia are too exaggerated and as an opposite consequence kill the organism like that in lipopolysaccharide (LPS)-induced septic shock in mice model and its amelioration in ASK1-deficient mice (MATSUZAWA *et al.* 2005).

We suggest that the cause of the phenotype of *nsy-1* mutant animals in anoxia is not ROS production by reoxygenation, first, because *nsy-1* mutant animals under oxidative stress showed not higher but rather lower survival rate (Figure 1A) and, second, because PMK-1 activation in response to anoxia was not suppressed by pretreatment with the ROS scavenger Nac (Figure 4D). Although the mechanism by which the NSY-1–SEK-1–PMK-1 pathway is activated remains unclear, a decrease in oxygen concentration might modify the extracellular or intracellular conditions and cause some damage to

the cell membrane such as that caused by a pore-forming toxin, which activates the unfolded protein response downstream of PMK-1 (Bischof *et al.* 2008).

In conclusion, the TIR-1–NSY-1–SEK-1–PMK-1 pathway is activated and regulates survival in anoxia. To elucidate the mechanism by which NSY-1 is activated by and responds to anoxia, we are currently screening factors that act upstream and downstream of the NSY-1–SEK-1–PMK-1 pathway using PMK-1 activity as a reporter.

We are grateful to R. Imae, T. Inoue, and the members of the Arai Laboratory for their technical support and input; to K. Kontani, M. Fukuyama, and the members of the Iino Laboratory for their technical advice and comments on this study; and to H. Moribe, T. Oka, G. M. Lesa, K. Gengyo-Ando, S. Mitani, and the Caenorhabditis Genetics Center for the provision of plasmids and strains. We thank all the members of the Laboratory of Cell Signaling for their helpful comments. This work was supported by grants-in-aid for scientific research from the Ministry of Education, Sciences, and Culture of Japan. T.H. was a research fellow of the Japan Society for the Promotion of Science.

LITERATURE CITED

Anderson, L. L., X. Mao, B. A. Scott and C. M. Crowder, 2009 Survival from hypoxia in *C. elegans* by inactivation of aminoacyl-tRNA synthetases. Science **323:** 630–633.

Bischof, L. J., C. Y. Kao, F. C. Los, M. R. Gonzalez, Z. Shen *et al.*, 2008 Activation of the unfolded protein response is required for defenses against bacterial pore-forming toxin in vivo. PLoS Pathog. **4:** e1000176.

Brahimi-Horn, M. C., and J. Pouyssegur, 2007 Oxygen, a source of life and stress. FEBS Lett. **581:** 3582–3591.

Brenner, S., 1974 The genetics of *Caenorhabditis elegans*. Genetics **77:** 71–94.

Chuang, C. F., and C. I. Bargmann, 2005 A Toll-interleukin 1 repeat protein at the synapse specifies asymmetric odorant receptor expression via ASK1 MAPKKK signaling. Genes Dev. **19:** 270–281.

Couillault, C., N. Pujol, J. Reboul, L. Sabatier, J. F. Guichou *et al.*, 2004 TLR-independent control of innate immunity in *Caenorhabditis elegans* by the TIR domain adaptor protein TIR-1, an ortholog of human SARM. Nat. Immunol. **5:** 488–494.

Dunwoodie, S. L., 2009 The role of hypoxia in development of the mammalian embryo. Dev. Cell **17:** 755–773.

Epstein, A. C., J. M. Gleadle, L. A. McNeill, K. S. Hewitson, J. O'Rourke *et al.*, 2001 *C. elegans* EGL-9 and mammalian homologs define a family of dioxygenases that regulate HIF by prolyl hydroxylation. Cell **107:** 43–54.

Ichijo, H., E. Nishida, K. Irie, P. ten Dijke, M. Saitoh *et al.*, 1997 Induction of apoptosis by ASK1, a mammalian MAPKKK that activates SAPK/JNK and p38 signaling pathways. Science **275:** 90–94.

Inoue, H., N. Hisamoto, J. H. An, R. P. Oliveira, E. Nishida *et al.*, 2005 The *C. elegans* p38 MAPK pathway regulates nuclear localization of the transcription factor SKN-1 in oxidative stress response. Genes Dev. **19:** 2278–2283.

Jiang, H., R. Guo and J. A. Powell-Coffman, 2001 The *Caenorhabditis elegans hif-1* gene encodes a bHLH-PAS protein that is required for adaptation to hypoxia. Proc. Natl. Acad. Sci. USA **98:** 7916–7921.

Kim, D. H., R. Feinbaum, G. Alloing, F. E. Emerson, D. A. Garsin *et al.*, 2002 A conserved p38 MAP kinase pathway in *Caenorhabditis elegans* innate immunity. Science **297:** 623–626.

Kondo, M., S. Yanase, T. Ishii, P. S. Hartman, K. Matsumoto *et al.*, 2005 The p38 signal transduction pathway participates in the oxidative stress-mediated translocation of DAF-16 to *Caenorhabditis elegans* nuclei. Mech. Ageing Dev. **126:** 642–647.

Lesa, G. M., M. Palfreyman, D. H. Hall, M. T. Clandinin, C. Rudolph *et al.*, 2003 Long chain polyunsaturated fatty acids are required for efficient neurotransmission in *C. elegans*. J. Cell Sci. **116:** 4965–4975.

Liberati, N. T., K. A. Fitzgerald, D. H. Kim, R. Feinbaum, D. T. Golenbock *et al.*, 2004 Requirement for a conserved Toll/interleukin-1 resistance domain protein in the *Caenorhabditis elegans* immune response. Proc. Natl. Acad. Sci. USA **101:** 6593–6598.

Mabon, M. E., X. Mao, Y. Jiao, B. A. Scott and C. M. Crowder, 2009 Systematic identification of gene activities promoting hypoxic death. Genetics **181:** 483–496.

Matsuzawa, A., K. Saegusa, T. Noguchi, C. Sadamitsu, H. Nishitoh *et al.*, 2005 ROS-dependent activation of the TRAF6–ASK1-p38 pathway is selectively required for TLR4-mediated innate immunity. Nat. Immunol. **6:** 587–592.

Mello, C. C., J. M. Kramer, D. Stinchcomb and V. Ambros, 1991 Efficient gene transfer in *C.elegans*: extrachromosomal maintenance and integration of transforming sequences. EMBO J. **10:** 3959–3970.

Mendenhall, A. R., B. LaRue and P. A. Padilla, 2006 Glyceraldehyde-3-phosphate dehydrogenase mediates anoxia response and survival in *Caenorhabditis elegans*. Genetics **174:** 1173–1187.

Menuz, V, K. S. Howell, S. Gentina, S. Epstein, I. Riezman *et al.*, 2009 Protection of *C. elegans* from anoxia by HYL-2 ceramide synthase. Science **324:** 381–384.

Moribe, H., J. Yochem, H. Yamada, Y. Tabuse, T. Fujimoto *et al.*, 2004 Tetraspanin protein (TSP-15) is required for epidermal integrity in *Caenorhabditis elegans*. J. Cell Sci. **117:** 5209–5220.

Nystul, T. G., J. P. Goldmark, P. A. Padilla and M. B. Roth, 2003 Suspended animation in *C. elegans* requires the spindle checkpoint. Science **302:** 1038–1041.

Oka, T., T. Toyomura, K. Honjo, Y. Wada and M. Futai, 2001 Four subunit a isoforms of *Caenorhabditis elegans* vacuolar H^+-ATPase. Cell-specific expression during development. J. Biol. Chem. **276:** 33079–33085.

Padilla, P. A., T. G. Nystul, R. A. Zager, A. C. Johnson and M. B. Roth, 2002 Dephosphorylation of cell cycle-regulated proteins correlates with anoxia-induced suspended animation in *Caenorhabditis elegans*. Mol. Biol. Cell **13:** 1473–1483.

Pei, B., S. Wang, X. Guo, J. Wang, G. Yang *et al.*, 2008 Arsenite-induced germline apoptosis through a MAPK-dependent, p53-independent pathway in *Caenorhabditis elegans*. Chem. Res. Toxicol. **21:** 1530–1535.

Powell-Coffman, J. A., 2010 Hypoxia signaling and resistance in *C. elegans*. Trends Endocrinol. Metab. **21:** 435–440.

Sagasti, A., N. Hisamoto, J. Hyodo, M. Tanaka-Hino, K. Matsumoto *et al.*, 2001 The CaMKII UNC-43 activates the MAPKKK NSY-1 to execute a lateral signaling decision required for asymmetric olfactory neuron fates. Cell **105:** 221–232.

Samokhvalov, V., B. A. Scott and C. M. Crowder, 2008 Autophagy protects against hypoxic injury in *C. elegans*. Autophagy **4:** 1034–1041.

Scott, B. A., M. S. Avidan and C. M. Crowder, 2002 Regulation of hypoxic death in *C. elegans* by the insulin/IGF receptor homolog DAF-2. Science **296:** 2388–2391.

Semenza, G. L., 2003 Targeting HIF-1 for cancer therapy. Nat. Rev. Cancer **3:** 721–732.

Shivers, R. P., T. Kooistra, S. W. Chu, D. J. Pagano and D. H. Kim, 2009 Tissue-specific activities of an immune signaling module regulate physiological responses to pathogenic and nutritional bacteria in *C. elegans*. Cell Host Microbe **6:** 321–330.

Shivers, R. P., D. J. Pagano, T. Kooistra, C. E. Richardson, K. C. Reddy *et al.*, 2010 Phosphorylation of the conserved transcription factor ATF-7 by PMK-1 p38 MAPK regulates innate immunity in *Caenorhabditis elegans*. PLoS Genet. **6:** e1000892.

Sifri, C. D., J. Begun, F. M. Ausubel and S. B. Calderwood, 2003 *Caenorhabditis elegans* as a model host for *Staphylococcus aureus* pathogenesis. Infect. Immun. **71:** 2208–2217.

Srinivasan, S., L. Sadegh, I. C. Elle, A. G. Christensen, N. J. Faergeman *et al.*, 2008 Serotonin regulates *C. elegans* fat and feeding through independent molecular mechanisms. Cell Metab. **7:** 533–544.

Sugimoto, A., 2006 RNAi by soaking, in *Reverse Genetics*, edited by J. Ahringer. WormBook, http://www.wormbook.org.

Takeda, K., T. Noguchi, I. Naguro and H. Ichijo, 2008 Apoptosis signal-regulating kinase 1 in stress and immune response. Annu. Rev. Pharmacol. Toxicol. **48:** 199–225.

Tanaka-Hino, M., A. Sagasti, N. Hisamoto, M. Kawasaki, S. Nakano *et al.*, 2002 SEK-1 MAPKK mediates Ca^{2+} signaling to

determine neuronal asymmetric development in *Caenorhabditis elegans*. EMBO Rep. **3:** 56–62.

Van Voorhies, W. A., and S. Ward, 1999 Genetic and environmental conditions that increase longevity in *Caenorhabditis elegans* decrease metabolic rate. Proc. Natl. Acad. Sci. USA **96:** 11399–11403.

Van Voorhies, W. A., and S. Ward, 2000 Broad oxygen tolerance in the nematode *Caenorhabditis elegans*. J. Exp. Biol. **203:** 2467–2478.

Wang, S., M. Tang, B. Pei, X. Xiao, J. Wang *et al.*, 2008 Cadmium-induced germline apoptosis in *Caenorhabditis elegans*: the roles of HUS1, p53, and MAPK signaling pathway. Toxicol.Sci. **102:** 345–351.

Communicating editor: D. I. Greenstein

GENETICS

Supporting Information
http://www.genetics.org/cgi/content/full/genetics.110.124883/DC1

Regulation of Anoxic Death in *Caenorhabditis elegans* by Mammalian Apoptosis Signal-Regulating Kinase (ASK) Family Proteins

Teruyuki Hayakawa, Kumiko Kato, Ryoichi Hayakawa, Naoki Hisamoto, Kunihiro Matsumoto, Kohsuke Takeda and Hidenori Ichijo

DOI: 10.1534/genetics.110.124883

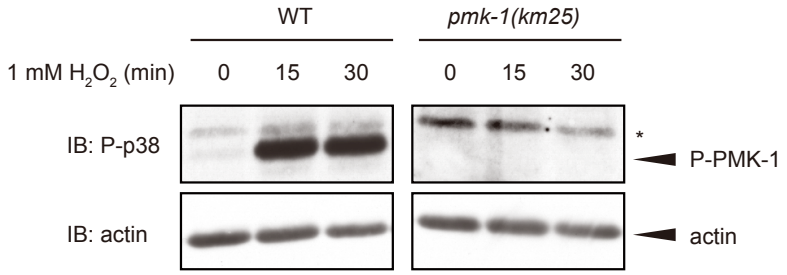

FIGURE S1.—Characterization of anti-phospho-p38 antibody in *C. elegans*. Wild-type (WT) and *pmk-1(km25)* mutant animals were stimulated by 1 mM of hydrogen peroxide (H_2O_2) for the indicated periods and were analyzed by immunoblotting (IB) using anti-phospho-p38 antibody. The band indicated by an arrowhead was completely abolished in *pmk-1(km25)* mutant. An asterisk indicates a non-specific band. The data shown are representative of two independent immunoblots.

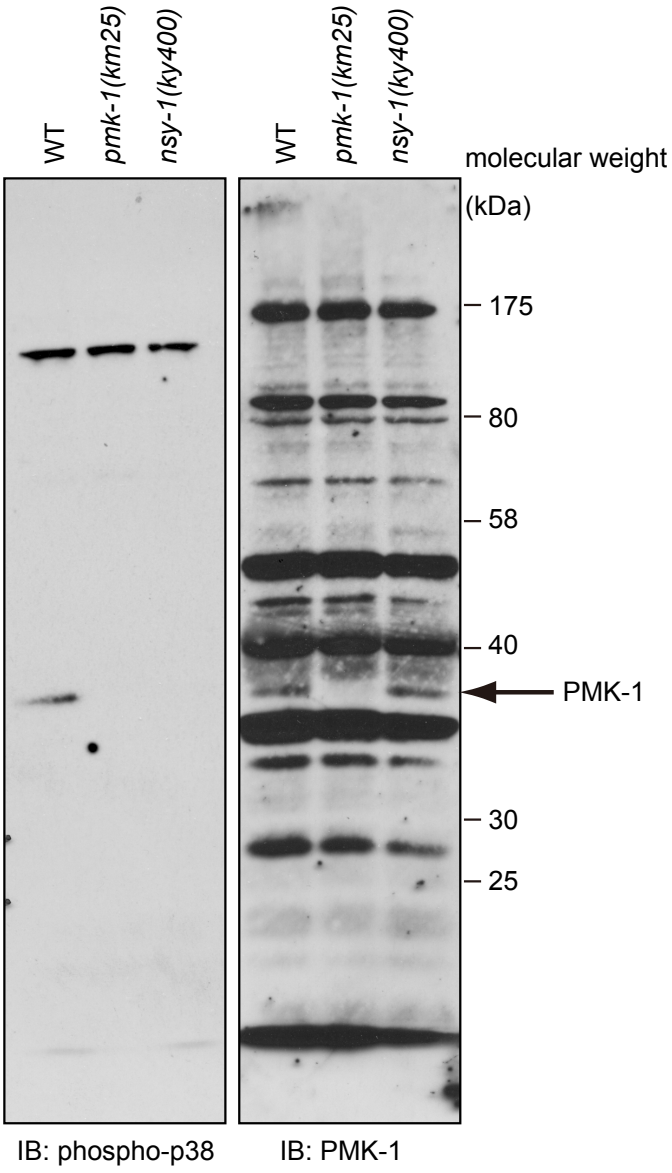

FIGURE S2.—Characterization of anti-PMK-1 antibody. Wild-type (WT), *pmk-1(km25)* and *nsy-1(ky400)* mutant animals were analyzed by immunoblotting (IB) using anti-phospho-p38 and anti-PMK-1 antibody. The arrow indicates the specific band for PMK-1.

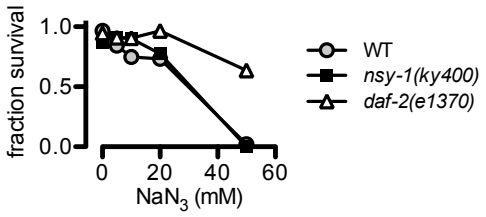

FIGURE S3.—Sodium azide sensitivity of the wild-type (WT), *nsy-1* and *daf-2* mutant animals. Approximately 100 synchronized young adult animals were incubated with various concentrations of sodium azide for 10 h. Twenty-four hours later, animals that moved spontaneously or responded to platinum wire touch were counted as surviving animals. The data shown are representative of five independent experiments.

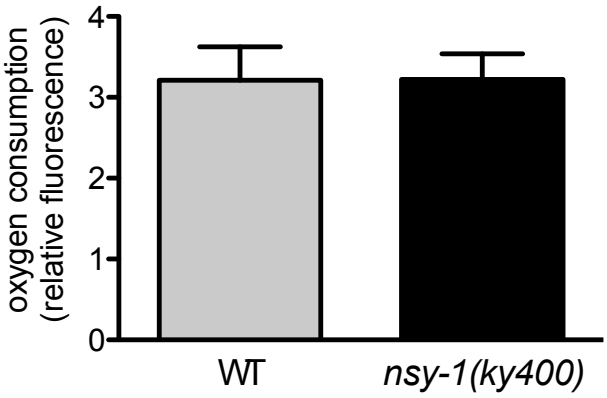

FIGURE S4.—Oxygen consumption rate of wild-type (WT) and *nsy-1* mutant animals. Synchronized young adult animals were harvested and oxygen consumption rates were measured using an Oxygen Biosensor System (BD). Data represent the mean (±SEM) oxygen consumption rate from four independent experiments. $p = 0.985$ by unpaired Student's *t*-test.